Chang Bonnie (Orcid ID: 0000-0002-5887-8655)

Title: Low rates of dinitrogen fixation in the eastern tropical South Pacific

Authors: Bonnie X. Chang[1,2*], Amal Jayakumar[3], Brittany Widner[4,5], Peter Bernhardt[5], Calvin W. Mordy[1,2], Margaret R. Mulholland[5], Bess B. Ward[3]

[1]Joint Institute for the Study of the Atmosphere and Ocean
University of Washington
Seattle, WA, USA

[2]Pacific Marine Environmental Laboratory/NOAA
Seattle, WA, USA

[3]Department of Geosciences
Princeton University
Princeton, NJ, USA

[4]Department of Marine Chemistry & Geochemistry
Woods Hole Oceanographic Institution
Woods Hole, MA, USA

[5]Department of Ocean, Earth and Atmospheric Sciences
Old Dominion University
Norfolk, VA, USA

*Corresponding author:
bxc@uw.edu
Joint Institute for the Study of the Atmosphere and Ocean
University of Washington
Box 355672
Seattle, WA 98195
USA

Running head: South Pacific dinitrogen fixation

Keywords: nitrogen fixation, eastern tropical South Pacific oxygen deficient zone, nitrogen cycle, bubble method

This is the author manuscript accepted for publication and has undergone full peer review but has not been through the copyediting, typesetting, pagination and proofreading process, which may lead to differences between this version and the Version of Record. Please cite this article as doi: 10.1002/lno.11159

Abstract

Recent work has suggested that the oxygen deficient zone (ODZ) and overlying surface waters of the eastern tropical South Pacific (ETSP) is a potential niche for dinitrogen (N_2) fixation. Rates of dinitrogen fixation were measured in the ETSP above and within the ODZ in July 2013 using a modified $^{15}N_2$ bubble addition method, wherein a bubble was added, mixed, and then removed, and the isotopic enrichment of the dissolved N_2 was measured directly for each incubation. N_2 fixation rates in the euphotic zone ranged from below detection to 3.9 nmol L^{-1} d^{-1} and were below detection at all depths surveyed within the ODZ. Depth-integrated rates ranged from below detection to 289.7 μmol m^{-2} d^{-1}. DNA and RNA of diverse *nifH* genes were detected at both surface waters and in the ODZ. However, the results of this study suggest that N_2 fixation rates were low and contribute little to N cycling in the ETSP.

Introduction

The ocean's ability to take up carbon dioxide (CO_2) via photosynthesis depends on the supply of bioavailable "fixed" nitrogen (N) (McElroy 1983). The major biological source and sink of N to marine systems are dinitrogen (N_2) fixation and denitrification/anammox, respectively (Codispoti et al. 2001), but the balance between sources and sinks is currently under debate (Gruber 2004; Codispoti 2007). Mass balances indicate that the ocean may be losing fixed N (Codispoti 2007), however

paleoceanographic evidence suggests that the marine N inventory has been at steady state since the last glacial-interglacial cycle (Kienast 2000). Errors in estimates of the magnitudes of the N_2 fixation source or denitrification/anammox sink may be one of the causes of this discrepancy.

Marine N_2 fixation estimates from geochemical proxies are usually larger than those estimated from direct measurements, suggesting that direct measurements may be missing significant N_2 fixation or that geochemical proxies overestimate marine fixed N loss (Mahaffey et al. 2005). Historically, the majority of N_2 fixation has been thought to occur in warm oligotrophic surface waters (Karl et al. 2002), with the highest rates found in the tropical Atlantic (Luo et al. 2014). However, recent work has shown that in the absence of oxygen (O_2) the energetic cost of N_2 fixation is comparable to that of nitrate (NO_3^-) uptake, indicating a possible niche for N_2 fixation within NO_3^--replete O_2-deficient waters (Großkopf and Laroche 2012). Additionally, analyses of distributions of N_2 fixation rates (Luo et al. 2014, Landolfi et al. 2018) and nutrient ratios (Deutsch et al. 2007) suggest that high rates of N_2 fixation may occur in the surface waters proximate to ODZs. Significant N_2 fixation geographically coupled to intense N-loss would provide a mechanism for feedbacks to maintain a balanced marine N budget through the last climatic oscillation, however there are still relatively few studies in this region (Luo et al. 2012) owing to the expectation that N_2 fixation would be limited by iron (Fe) given the low dust fluxes to this region (Moore et al. 2004; Dutkiewicz et al. 2012).

Previous direct estimates of N_2 fixation from the ETSP reported areal rates comparable to those found in oligotrophic gyres (117 μmol N m^{-2} d^{-1}, Bonnet et al. 2013), to 800 μmol N m^{-2} d^{-1} at a single sulfidic station (Loescher et al. 2014). Indirect rates estimated from sediment trap fluxes are much lower (≤23 μmol N m^{-2} d^{-1}, Knapp et al., 2016). Significant rates of N_2 fixation and diverse *nifH* genes have been reported from both the euphotic zone (Dekaezemacker et al. 2013) and the ODZ (Fernandez et al. 2011; Löscher et al. 2016) in the ETSP. The presence and expression of *nifH* genes implies the activity of diverse diazotrophs in both surface and ODZ waters, but accurate measurements of N_2 fixation rates are necessary in order to determine the contributions of these diazotrophs to the C and N cycles and to resolve the discrepancy in the oceanic N inventory.

Marine N_2 fixation rates may also be underestimated due to methodological bias. The widely used $^{15}N_2$ incorporation method (i.e. "bubble method", Montoya et al. 1996) has been found to underestimate N_2 fixation rates by up to 6-fold (Mohr et al. 2010; Großkopf et al. 2012), although a recent experimental comparison suggests a much smaller discrepancy between methods (Wannicke et al. 2018). A new method has been proposed to address this issue, which uses $^{15}N_2$ tracer pre-equilibrated with seawater (Mohr et al. 2010; Klawonn et al. 2015); however, this method can be impractical when measuring N_2 fixation rates at multiple depths in the field where biogeochemical gradients can be profound.

In this study we assessed the distribution and magnitude of N_2 fixation above and within the ETSP ODZ, along with the diversity, abundance, and transcription of *nifH*, a key gene in the N_2 fixation process. We measured N_2 fixation rates at stations in the ETSP ranging from nutrient replete coastal upwelling to offshore stations where dissolved inorganic N (DIN) concentrations were <1 μM. Depth profiles encompassed both the oxic euphotic zone and the aphotic ODZ. To measure N_2 fixation rates we used a modified bubble method (Klawonn et al. 2015), which avoids the underestimation problem of the classic bubble method (Montoya et al. 1996).

Materials and methods

Study site and hydrographic parameters

Water samples were collected from 7 stations in the ETSP ODZ in June/July 2013 aboard the R/V Nathaniel B. Palmer (Fig. 1). Five of those stations (Sta. 2, BB1, 9, 10, and 16) were offshore (>370 km from the coastline between 13 and 21°S), and 2 stations (Sta. 21 and BB2) were nearshore (<50 km from the coast between 20 and 22°S). Profiles of O_2 were measured using a SBE 43 O_2 sensor, calibrated by Winkler titrations of discrete samples. Nitrate (NO_3^-), nitrite (NO_2^-), and ammonium (NH_4^+) concentrations were measured onboard using automated continuous flow analysis with a segmented flow and colorimetric detection following standardization and analysis procedures by Gordon

et al. (1994). Detection limits for NO_3^-, NO_2^-, and NH_4^+ were 0.07, 0.02, and 0.04 μM, respectively.

N_2 fixation rates

Water for N_2 fixation incubations was collected directly from Niskin bottles mounted on a CTD rosette into triplicate acid-cleaned incubation vessels. Between 2 and 5 euphotic zone depths and 0 and 6 ODZ depths were sampled at each station. Whole water samples from the euphotic zone were collected from pre-dawn casts and incubated in 2.5 L acid-washed PETG bottles fitted with septa caps. Whole water samples from the ODZ were transferred to transparent acid-washed (10% HCl), helium (He)-purged, evacuated, 2-mil polyvinyl fluoride (PVF) gas-tight 5 L Tedlar bags with dual entry points: one a nickel-plated brass hose barb and the other a septum (Cole Parmer, EW-01409-92) using inert tubing attached to the hose barb, and any remaining He was removed from the bags via syringe attached to the septum during filling. Atmospheric O_2 contamination during water collection was minimized by continually flushing the headspace of Niskin bottles with He. Initial particulate N concentrations and isotopic composition (atom%) were determined in triplicate for each depth by filtering whole water onto 25 mm GF/F filters (nominal pore size 0.7 μm).

A widely used method to directly measure N_2 fixation rates ("bubble method", Montoya et al. 1996) has been found to significantly underestimate N_2 fixation rates in

individual incubations (Mohr et al. 2010; Großkopf et al. 2012). The addition of seawater, which has been pre-equilibrated with $^{15}N_2$, to incubations has been proposed as a more accurate method of introducing $^{15}N_2$ tracer ("dissolution method", Mohr et al. 2010). However, this approach requires substantial manipulations to filter, degas, and enrich seawater, which likely alters the chemical composition of the $^{15}N_2$-enriched seawater and has unknown effects on the microbial community. The most obvious alteration is that degassing removes carbon dioxide, causing a large change in pH and resulting in precipitation of calcium carbonate. The production of pre-equilibrated seawater is also time-consuming such that it is difficult to produce sufficient quantities of pre-equilibrated site water in a short enough time period.

The modified bubble method (Klawonn et al. 2015) used in this study avoids the deficiencies of both the original bubble method and the dissolution method. It allows for initiation of incubations quickly after collection of sample water, minimizing perturbations to the in situ microbial community, and the atom% $^{15}N_2$ in incubations remains stable for the duration of the incubation (Fig. S1). $^{15}N_2$ tracer (99%, Cambridge Isotope Labs) was injected into bottles and bags through the septa to a target concentration of ~10% ambient N_2 (1 mL $^{15}N_2$ per liter of incubation). Bottles and bags were gently inverted and shaken, respectively, for 15 min, after which the $^{15}N_2$ bubble was removed and, in bottles, replaced with site water such that there was no headspace.

In order to determine the atom% enrichment of the dissolved N_2 in each

incubation vessel, duplicate 6 mL subsamples were transferred from each incubation bottle or bag at the end of the incubation into He-purged 12 mL Exetainers (Labco) which were immediately poisoned with 0.05 mL 7 M zinc chloride ($ZnCl_2$). Up to two additional timepoints for $^{15}N_2$ were collected in duplicate from select bottles and bags to confirm that the atom% $^{15}N_2$ remained consistent over the course of the incubation. To sample $^{15}N_2$ timepoints, bottles were left capped and a 15 cm needle was used to slowly withdraw volume through the septa while a 1 cm needle was used to replace withdrawn volume with site water. Samples were corrected for dilution due to the addition of site water, which resulted in an average decrease of 0.04 atom% $^{15}N_2$ per timepoint. Exetainers were analyzed for atom% $^{15}N_2$ on a Europa 20/20 isotope ratio mass spectrometer (IRMS) equipped with a copper reduction furnace heated to 500°C to remove O_2. O_2 is problematic in that it can recombine with unlabeled N_2 in the ion source of the mass spectrometer to form NO^+, which has a mass indistinguishable from doubly labeled $^{15}N_2$ (Eyre et al. 2002).

Euphotic zone samples were incubated for approximately 24 h in flow-through incubators on deck. In situ light levels, estimated from the CTD PAR data, were simulated using neutral density screens. Near surface water temperatures were maintained with flowing surface seawater. ODZ samples were incubated for approximately 24 h in a 12°C cold room (in situ temperature range of ODZ samples: 9.8 – 13.7°C) in the dark.

Incubations were terminated by filtering the entire contents of the incubations onto pre-combusted (450°C for 2 h) 25 mm GF/F filters (nominal pore size 0.7 μm). Filters were stored at -20°C, then dried and pelletized in tin discs and analyzed for isotopic enrichment on a Europa Geo 20/20 IRMS equipped with an automated N and C analyzer. To characterize and correct for the effect of a non-linear detector response to varying sample size (McIlvin & Casciotti 2010), known standards of different sample masses were run (1.17 – 100 μg N), bracketing the sample masses (2.0 – 38.9 μg N). The limit of detection of the instrument was approximately 1 μg N.

Rates of N_2 fixation were calculated using equation (1):

$$N_2 \text{ fixation rate} = \frac{\left(A_{PN}^{final} - A_{PN}^{t=0}\right)}{\left(A_{N_2} - A_{PN}^{t=0}\right)} \times \frac{[PN]}{\Delta t} \qquad (1),$$

where A = atom% ^{15}N measured in the particulate organic N (PN) at the end (final) or beginning (t = 0, initial) of the incubation or in the dissolved N_2 pool (N_2) (Montoya et al. 1996, Mulholland et al. 2006).

The method detection limit was calculated following Ripp (1996). Briefly, the standard deviation of the atom% from seven standards of 12 μg N each (0.0008%) was multiplied by three (0.0025%) and added to the initial atom% measurement for each sample. This was the minimum detectable final particulate atom% enrichment. This value was then forced through the calculation for each measurement to account for variability in particulate nitrogen concentrations with depth and incubation times, resulting in an independent detection limit for each measurement. The average detection limit for oxic

incubations was higher than for anoxic incubations (0.6 and 0.3 nmol N L^{-1} d^{-1}, respectively), due to higher particulate organic nitrogen concentrations in the euphotic zone compared to the ODZ. If 2 out of 3 replicates were below detection, the average of 3 replicates was forced to zero (Bonnet et al. 2013).

NifH gene analysis

Particulate material from multiple casts from Sta. BB1 and BB2 (Fig. 1) was collected for *nifH* diversity and abundance analysis. For *nifH* gene abundance seven samples from Sta. BB1 and 11 samples from Sta. BB2, covering the depth range between surface and 1000 m, were collected. *nifH* clone libraries for DNA and cDNA were analyzed at two depths each at Sta. BB1 and BB2: near surface (0 – 20 m) and the secondary nitrite maximum depth at both stations (130 m at Sta. BB1 and 115 m at Sta. BB2). Whole water (4 – 8 L) from CTD-mounted Niskin bottles was filtered through Sterivex-GP capsule filters (pore size 0.2 μm, Millipore), using a peristaltic pump, flash frozen in liquid nitrogen, and shipped in a dry shipper to Princeton University. The samples were stored at -80^{o}C until DNA and RNA were extracted.

DNA and RNA were simultaneously extracted from Sterivex filters using the ALLPrep DNA/RNA Mini Kit (Qiagen). cDNA was synthesized immediately following purification of RNA using a SuperScript III First Strand Synthesis System (Invitrogen, Carlsbad, CA, USA) following the procedure described by the manufacturer. DNA was

quantified using PicoGreen dsDNA quantification kit (Invitrogen) according to the manufacturer's specifications. *nifH* sequences were amplified from environmental DNA and cDNA using a Promega PCR kit, on an MJ100 Thermal Cycler (MJ Research). A nested reaction was used, as previously described (Zehr et al. 1998), with slight modification: 25 μl PCR reactions were amplified for 30 cycles (1 min at 98°C, 1 min at 57°C, 1 min at 72°C), first with the outer PCR primers (Zani et al. 2000), followed by amplification with the inner PCR primers (Zehr & McReynolds 1989). In order to minimize the possibility of amplifying contaminants (Zehr et al. 2003), negative controls (autoclaved and UV-irradiated water) were run with every PCR experiment, reagents were diluted in freshly autoclaved water, the PCR preparation station was UV irradiated for 1 hour before each daily use and the number of cycles was limited to 30 for each reaction. The PCR reagents (except components sensitive to irradiation) were also irradiated and were then tested separately for amplification in negative controls.

Amplified fragments were electrophoresed on 1.2% agarose gels and *nifH* bands were excised and then cleaned using a QIAquick Nucleotide Removal Kit (Qiagen). Cleaned fragments were inserted into a pCR®2.1-TOPO® vector using One Shot® TOP10 Chemically Competent *E. coli*, TOPO TA Cloning® Kit (Invitrogen) according to manufacturer's specifications. This resulted in a total of 8 clone libraries.

Clones were picked randomly and amplified using M13 Forward (-20) and M13 Reverse primers. The products were sequenced at the Macrogen DNA Analysis Facility

using Big DyeTM terminator chemistry (Applied Biosystems, Carlsbad, CA, USA). Sequences were edited using FinchTV ver. 1.4.0 (Geospiza Inc.) and checked for identity using BLAST. Consensus *nifH* sequences (359 bp) were translated to amino acid (aa) sequences (108 aa after trimming the primer region) and aligned using ClustalX (Thompson et al. 1997) along with published *nifH* sequences from the NCBI database. Neighbor-joining trees were produced from the alignment using distance matrix methods (PAUP 4.0, Sinauer Associates). Bootstrap analysis was used to estimate the reliability of phylogenetic reconstruction (1000 iterations). The *nifH* sequence from *Methanosarcina lacustris* (AAL02156) was used as an outgroup.

The *nifH* nucleotide alignment (of 258 sequences) was used to define operational taxonomic units (OTUs) on the basis of DNA sequence identity. Distance matrices based on this nucleotide alignment were generated in MOTHUR (Schloss et al. 2009). OTUs were defined as of sequences which differed by ≤ 5 % using the furthest neighbor method in the MOTHUR program (Schloss et al. 2009).

The new ETSP *nifH* sequences have been deposited in GenBank, DNA sequences accession numbers MK408165 – MK408307 and cDNA sequences accession numbers MK408308 – MK408422.

Standardization and verification of specificity for Q-PCR assays was performed as described in Jayakumar et al. (2009). Primers nifHfw and nifHrv (Mehta et al. 2003, Dang et al. 2013) forward 5-GGHAARGGHGGHATHGGNAARTC-3 and reverse 5-

GGCATNGCRAANCCVCCRCANAC-3, which correspond to the amino acid positions 10 to 17 (GKGGIGKS) and 132 to 139 (VCGGFAMP) of *Klebsiella pneumoniae* numbering, (Mehta et al. 2003) were used (100 pmoles per 25 mL reaction) to amplify a ~400 bp region of the *nifH* gene for *nifH* quantification. Assays were carried out with Qiagen master mix (Qiagen Sciences, Maryland, USA) at an annealing temperature of 56 °C. These conditions were chosen based on amplification efficiency and reproducibility of results with a single product, after running test assays on a Stratagene MX3000P (Agilent Technologies, La Jolla, CA, USA). The amplified products were visualized after electrophoresis in a 1.0% agarose gel stained with ethidium bromide. Standards for quantification were prepared by amplifying a constructed plasmid containing the *nifH* gene fragment, followed by quantification and serial dilution. Assays for all depths were carried out in a single assay plate (Smith et al. 2006). Each assay included triplicates of the no template controls (NTC), no primer control (NPR), four or more standards, and known quantity of the environmental DNA samples. A subset of samples from the previous run was included in subsequent assays, as well as a new dilution series for standard curves on every assay. These new dilution series were produced immediately following re-quantification of plasmid DNA concentrations to verify gene abundance (because concentrations declined upon storage and freeze–thaw cycles). Automatic analysis settings were used to determine the threshold cycle (Ct) values. The copy numbers were calculated according to equation (6):

$$\text{copy number} = \frac{\text{ng} \times \frac{\text{number}}{\text{mole}}}{\text{bp} \times \frac{\text{ng}}{\text{g}} \times \frac{\text{g}}{\text{mole bp}}} \qquad (6),$$

and then converted to copy number mL^{-1} seawater filtered. An extraction efficiency of 100% was assumed, meaning that the results could be underestimates of the true value.

Results

Hydrographic conditions

The stations sampled for N_2 fixation rate experiments were grouped into three regimes based on euphotic zone and ODZ hydrochemistry (Fig. 2, Table 1): ODZ margin (Sta. 2 and 10), offshore ODZ (Sta. BB1, 9, and 16), and coastal ODZ (Sta. 21 and BB2). For stations on the ODZ margin, the anoxic layer was <30 m), there was no detectable secondary NO_2^- maximum (SNM), and [DIN] was low in the euphotic zone. Stations in the offshore ODZ were characterized by a thick anoxic layer (~250 m), [NO_2^-] exceeded 7 μM at the SNM, and [DIN] in the euphotic zone at the offshore ODZ stations was higher than at the ODZ margin stations. Stations in the coastal ODZ had the thickest anoxic layer (~330m) with [NO_2^-] exceeding 7 μM at the SNM, and [DIN] in the euphotic zone was the highest of the 3 regimes.

Stations along the ODZ margin and in the offshore ODZ were situated outside the most intense coastal upwelling region, as is evidenced by sea surface temperature (Fig. 1 in Widner et al. 2018). Surface chlorophyll *a* concentrations were also lower at the ODZ

margin (0.1 – 0.4 mg m^{-3}) and offshore ODZ (0.1 – 2.3 mg m^{-3}) stations than at the coastal stations (0.3 – 5.6 mg m^{-3}) (Fig. 1, Table 1).

Atom% $^{15}N_2$ in incubations and initial PN

In incubations of water from the ETSP ODZ, atom% $^{15}N_2$ achieved using the modified bubble method ranged from 2.3 to 6.9 in PETG bottles and from 0.8 to 9.0 in Tedlar bags. The average standard deviation of duplicate Exetainer samples collected from the same bottle or bag was 0.1 atom% $^{15}N_2$ (n=173). In bottles where samples for determination of atom% $^{15}N_2$ were taken at 2 to 3 timepoints (Fig. S1), the average standard deviation between samples from all timepoints of a given incubation was 0.3 atom% $^{15}N_2$ (n = 37).

Average initial atom% ^{15}N–PN in ODZ incubations (0.3707±0.0012 atom%) was enriched relative to euphotic zone incubations (0.3689±0.0008 atom%) (Fig. S2). Average initial atom% ^{15}N–PN in all incubations was enriched relative to atmospheric N_2 (0.3663 atom%). Ambient [PN] (t = 0, initial) in the water column was highest in the euphotic zone (0.3 – 1.8 μM N) and decreased with increasing depth (range of ODZ [PN] 0.1 – 0.6 μM N) (Fig. S2).

N_2 fixation rates

N_2 fixation was detected in 6 samples collected from oxic euphotic waters at 3 of the 7 stations sampled in the ETSP (Fig. 2) but was not detected in ODZ waters below. The highest rates of N_2 fixation (1.6±0.4 to 3.9±1.6 nmol N L^{-1} d^{-1}) were found at Sta. 2, outside the coastal upwelling zone and where surface DIN and chlorophyll *a* concentrations were relatively low (Figs. 1 and 2). In contrast, rates of N_2 fixation were lower in surface waters at Sta. BB1 (0.7±0.2 nmol N L^{-1} d^{-1}) and Sta. BB2 (0.9±0.5 to 1.1±0.04 nmol N L^{-1} d^{-1}) where DIN and chlorophyll *a* concentrations were slightly higher than at Sta. 2. N_2 fixation rates were below the limit of detection in samples collected from the anoxic zone at all 7 total stations. Depth integrated N_2 fixation rates were 289.7 μmol N m^{-2} d^{-1} at Sta. 2 (from surface to 275 m), 4.2 μmol N m^{-2} d^{-1} at Sta. BB1 (from surface to 350 m), and 23.0 μmol N m^{-2} d^{-1} at Sta. BB2 (from surface to 240 m).

Commercial $^{15}N_2$ stocks are potentially contaminated with ^{15}N-enriched NO_3^-, NO_2^-, and NH_4^+, which may be assimilated by microbes leading to an overestimate of N_2 fixation rates (Dabundo et al. 2014). We calculated the N_2 fixation rate that would have been inferred from the uptake of ^{15}N contaminants using the same finite-differencing model approach as Dabundo et al. (2014) (see SI) and found the rates of N_2 fixation inferred from the potential uptake of ^{15}N contaminants (-0.05 – 0.01 nmol N L^{-1} d^{-1}) below the calculated detection limits in all cases.

Distribution of *nifH* genes

QPCR analysis detected between 1.2 x 10^4 and 5.3 x 10^4 *nifH* genes mL^{-1} in the surface mixed layer (Fig. 3). Gene abundances were lower within the ODZ and varied between ~40 and ~10^4 mL^{-1} of seawater. The profiles of *nifH* abundance were similar between the two stations, with highest abundance in the surface waters and a smaller secondary peak at the depth of the SNM in the core of the ODZ.

NifH diversity

NifH clone libraries from the ODZ (SNM) and surface layer depths from two stations, both DNA and cDNA resulted in the generation of 258 *nifH* sequences. Retrieved sequences belonging to Cluster I included only α- and γ- Proteobacteria; no cyanobacterial or β-Proteobacterial sequences were retrieved. Sequences belonging to Clusters III and IV, but not Cluster II, were also retrieved. Both DNA and cDNA sequences were detected at all four depths. In a few cases, identical DNA and cDNA sequences were found, but they were never from the same depth (e.g., DNA from Sta. BB2 20 m and cDNA from Sta. BB2 115m).

OTU analysis detected four OTUs in Cluster I and seven OTUs in Clusters III and IV combined. This is a relatively low overall diversity, as can be seen from the clustering of most of the sequences in a few branches of the phylogenetic trees (Fig. S3a and b).

Cluster I: Ninety-seven of the 127 Cluster 1 sequences from surface layer and SNM depths in the ETSP were identified as α–Proteobacteria and many were 99% identical to *Bradyrhizobium* spp. This clade was also found in the ODZ depths of the Arabian Sea (Jayakumar et al. 2012) and the ETNP (Jayakumar et al. 2017) and also in other sedimentary environments. Fifteen of the α–Proteobacterial cDNA sequences from Sta. BB2 ODZ clustered with *nifH* from *Methylocyctis rosea* SV97. The γ–Proteobacterial sequences were related to *Vibrio diazotrophicus*, *Marinobacterium luminaris*, and *Pseudomonas stutzeri*. All these DNA sequences clustered with environmental sequences from the Arabian Sea, South China Sea and oligotrophic waters from near the Bahamas. No sequences with high identities with any cultured species were found among the γ–Proteobacterial sequences in these samples.

Clusters III and IV: Only 36 sequences from this study grouped in Cluster III, which included DNA sequences derived from the surface depth of both Sta. BB1 and BB2, and cDNA sequences from Sta. BB2 ODZ depth. These sequences were closely related to sequences obtained from ODZ waters of the ETSP by Fernandez et al. (2011), and also environments including Chesapeake Bay, Norwegian Fjord, and the Black Sea. A small subgroup of Cluster III sequences included one cDNA sequence from Sta. BB2 ODZ depth and a DNA sequence from Sta. BB1 surface sample, and was 100% identical to DNA and cDNA sequences obtained from the ETNP surface waters and sequences

obtained from marine sponges and a Norwegian Fjord. This group also had a sequence obtained from Rongcheng Bay sediment.

Seventy-four sequences obtained from this study grouped in Cluster IV; these included predominantly DNA sequences from the offshore Sta. BB1, from both the surface and SNM. These sequences were 100% identical to DNA sequences from the ETNP ODZ (Jayakumar et al. 2017) and ETSP ODZ (direct NCBI submission, Accession number AMR73498). Another sub-group in Cluster IV included both DNA and cDNA sequences, identical to each other and closely related to a clone obtained from the Southwest Pacific Ocean, Solomon and Bismarck Seas (Benavides et al. 2015). One group of 30 cDNA sequences in Cluster IV from the surface waters of Sta. BB1 had close identities to *Rhodopseudomonas palustris*.

Discussion

Initial atom% ^{15}N of PN in incubations

With the recognition that N_2 fixation may occur in environments outside of the tropical surface ocean, more measurements are being carried out in environments where the ambient atom% ^{15}N–PN may vary significantly from the atom% of atmospheric N_2. Assuming the initial atom% ^{15}N–PN is equivalent to the isotopic composition of atmospheric N_2 can lead to the calculation of erroneous N_2 fixation rates (e.g. Bonnet et al. 2013). Voss et al. (2001) found the atom% ^{15}N–PN in the eastern tropical North

Pacific (ETNP) to be consistently higher in the ODZ relative to the overlying mixed layer, potentially as a result of trophic processing of PN by heterotrophs, which leaves behind PN relatively enriched in ^{15}N. In this study, average initial/ambient atom% ^{15}N–PN in the ETSP ODZ (0.3707±0.0012) was higher than the atom% ^{15}N–PN in the overlying euphotic zone (0.3689±0.0008 atom%), and initial atom% ^{15}N–PN in all incubations were higher than atmospheric N_2 (0.3663 atom%) (Fig. S2). If initial atom% ^{15}N–PN was assumed to be the same as atom% ^{15}N of atmospheric N_2, N_2 fixation rates calculated in this study would be erroneously higher than if the measured initial atom% ^{15}N–PN was used. Even relatively small increases in volumetric rates could result in substantially higher depth/area integrated N_2 fixation rates.

N_2 fixation rates in the ETSP

The low number of detectable nitrogen fixation rates indicates that N_2 fixation in and above the ETSP ODZ is either sparse, temporally/spatially heterogeneous, or both. Previous work by other researchers shows that N_2 fixation in this region can be patchy (Dekaezemacker et al. 2013; Loescher et al. 2014; Fernandez et al. 2015), potentially a reflection of the sporadic availability of organic matter which may fuel heterotrophic N_2 fixing microbes in the ODZ. Given the relatively small number of detectable rates in this study, it is difficult to draw detailed conclusions regarding the magnitude and controls of N_2 fixation in this region. However, as there are relatively few studies of pelagic N_2

fixation outside of warm, N-deplete environments (Landolfi et al., 2018), it is interesting to examine these results more closely.

When detected, volumetric rates of N_2 fixation in the euphotic zone were modest (1.6 – 3.9 nmol N L^{-1} d^{-1} at Sta. 2, 0.7 nmol N L^{-1} d^{-1} at Sta. BB1, and 0.9 – 1.1 nmol N L^{-1} d^{-1} at Sta. BB2) and comparable to previous studies in this region (Fernandez et al. 2011; Dekaezemacker et al. 2013; Bonnet et al. 2013; Loescher et al. 2014). Although, these previous studies used the "bubble method" (Montoya et al. 1996), which has been found to underestimate N_2 fixation rates, spatial and temporal heterogeneity are probably substantial enough to mask this difference. Recent work in the ETNP ODZ detected similarly low rates of N_2 fixation in surface waters of the ETNP, and found low but significantly non-zero rates at five out of 18 samples from ODZ depths (Jayakumar et al. 2017).

Previous estimates of areal N_2 fixation rates in this region span a wide range (undetectable to 622 μmol m^{-2} d^{-1}), driven both by variable volumetric rates and by the consideration of depth intervals ranging from the euphotic zone only (i.e. Dekaezemacker et al. 2013) to 2000 m (Bonnet et al. 2013). In this study, volumetric rates were integrated to 240 – 350 m, well into or at the bottom of the ODZ. However, since no detectable rates were found below the euphotic zone, functionally the areal rate represents the euphotic zone only. Areal rates at Sta. BB1 and BB2 (4.2 and 23.0 μmol m^{-2} d^{-1}, respectively) are similar to studies in this region that consider only the euphotic zone (Dekaezemacker et

al. 2013; Knapp et al. 2016). Sta. 2 is an exception, having a high areal rate (289.7 μmol m^{-2} d^{-1}), comparable to values obtained in tropical, oligotrophic regions (Luo et al. 2014).

Failure to detect N_2 fixation below the euphotic zone of the ETSP could also be due to loss during filtration of smaller unicellular diazotrophs (γ–Proteobacteria) that were detected by *nifH* gene analysis in the anoxic layer. Bombar et al. (2018) compared the effect of pore size (0.7 vs. 0.3 μm pore size glass fiber filters) on N_2 fixation rates measured using the dissolution method (Mohr et al. 2010) in three estuarine and marine environments. Significant N_2 fixation rates were detected in six samples, and for half of those, the rates were higher on the smaller filter size. To investigate the effect of filter pore size on the measured rate, i.e., to determine if the GF/F filters missed smaller cells that might have been fixing N_2, [PN] and N_2 fixation rates were compared on GF/F (nominal pore size 0.7 μm) and silver (pore size 0.2 μm) filters in bag incubations carried out at 19 ODZ depths at 7 stations in the eastern tropical North Pacific (ETNP) ODZ in 2012 (see SI). At values less than ~1.5 μmol N L^{-1}, [PN] on each filter type was comparable (Fig. S4a). At higher [PN], GF/F filters retained more PN relative to silver filters (Fig. S4a), likely due to the adsorption of dissolved organic N onto GF/F filters (Moran et al. 1999, Turnewitsch et al. 2007). Despite that mass difference, there was no pattern in the N_2 fixation rates measured on the two filter types (Fig. S4b). The highest rate was detected on the GF/F filters but the uncertainty in the low rates precludes detection of any significant differences between filter types. The filter size comparison

reported here was performed in the ETNP, and thus may not be directly applicable to interpretation of rates measured in the ETSP. Measured rates were negligible to very low in both locations, however, and it seems unlikely that filter pore size would change the results significantly.

N_2 fixation in the presence of dissolved inorganic N

There were detectable, and in some cases substantial (>1 μM), concentrations of NO_3^-, NO_2^-, and NH_4^+ at all depths at which N_2 fixation was also detected (Fig. 2 and 4). Historically N_2 fixation studies have concentrated on N-deplete waters, in part due to the high energetic cost of fixing N_2 compared to assimilating NO_3^- or NH_4^+ (Mulholland et al. 2001) although culture (Mulholland et al. 2001; Dekaezemacker and Bonnet 2011; Knapp et al. 2012) and field studies (Mulholland et al. 2012; Loescher et al. 2014, Fernandez et al. 2015) have demonstrated that N_2 fixation can occur in the presence of DIN (Sohm et al. 2011 and references therein).

In the current study, although N_2 fixation was detected in the presence of DIN, the highest rates of N_2 fixation were observed at the station with the lowest NO_3^- concentrations (0.6 – 0.9 μM at Sta. 2 compared to 2.6 μM at Sta. BB1 and 2.7 – 17.6 μM at Sta. BB2, Fig. 2 and 4). Concentrations of NH_4^+ were also slightly lower at Sta. 2 (0.08 – 0.14 μM) compared to Sta. BB1 (0.19 μM) and BB2 (0.17 – 0.31 μM).

Contribution of N_2 fixation to N utilization in the ETSP

The rates of N_2 fixation in the ETSP euphotic zone were also a very small fraction of total fixed N uptake at Sta. BB1 and 9. At Sta. BB1, Widner et al. (2018) reported total N (NO_3^- + NO_2^- + NH_4^+ + urea + cyanate) uptake rates of 348±26.4 and 368±104 nmol L^{-1} d^{-1} at the surface and 30 m depth, respectively, compared to N_2 fixation rates measured in this study of 0.7±0.2 nmol N L^{-1} d^{-1} at the surface and undetectable at 30 m depth. At Sta. 9, Widner et al. (2018) measured total N uptake rates of 498±134 and 279±82.0 nmol L^{-1} d^{-1} at the surface and 30 m depth, respectively, compared to undetectable N_2 fixation rates found in this study at that station. This suggests that fixed N requirements for phytoplankton at Sta. BB1 and 9 were largely fulfilled by existing sources of fixed N, not by N_2 fixation. This finding corroborates Knapp et al. (2016), who concluded N_2 fixation was a minor contributor to new/export production in the ETSP.

NifH phylogeny and abundance

The phylogenetic distribution of diazotrophs detected in this study is consistent with that reported previously by Turk-Kubo et al. (2014) in the ETSP – the assemblage was dominated by γ–Proteobacteria and none of the usual cyanobacterial clades were detected. All of the *nifH* sequences reported here were most closely related to sequences usually associated with heterotrophic or methylotrophic bacteria.

The highest abundance of nifH genes reported here is higher than that reported in previous studies of non-cyanobacterial *nifH* genes (Moisander et al. 2017) and were found only in surface waters. These values are substantially higher than those reported by Turk-Kubo et al. (2014) from further offshore in the same regions, and somewhat higher than those reported by Loescher et al. (2014) for coastal ETSP waters. Both of those studies used clade or cluster specific PCR primers, while wide spectrum general primers were used in the present study. Thus the abundances reported here may represent a wider diversity than detected with the more specific primers used in previous studies.

The depth distribution of diazotrophs estimated from qPCR was similar to the distribution of nitrogen fixation rates with the highest gene abundance in surface waters. The depth resolution of the gene abundance and chemical profiles was not sufficient to link the gene abundance maxima directly to the chemical distributions, but the secondary gene abundance maximum clearly falls within the core of the ODZ within the secondary nitrite maximum and the nitrate deficit. This deep maximum in *nifH* gene abundance was not reflected in N_2 fixation rates, which were not detectable at these depths. Thus, even though the organisms responsible for N_2 fixation are present and active (i.e., expressing the *nifH* genes) in the study area, they are not associated with significant production of new N.

Acknowledgements

The authors are grateful for the help provided by the captain and crew of the *R/V Nathanial B. Palmer*. This work was funded by NSF grant no. OCE-1029951 to B.B.W. and A.J., and NSF grant no. OCE-1356043 to M.R.M., A.J. and B.X.C. This publication is partially funded by the Joint Institute for the Study of the Atmosphere and Ocean (JISAO) under NOAA Cooperative Agreement NA15OAR4320063, Contribution No. 2018-0172. This is NOAA-PMEL contribution no. 4862.

References

Benavides, M., P. H. Moisander, H. Berthelot, T. Dittmar, O. Grosso, and S. Bonnet. 2015. Mesopelagic N_2 Fixation Related to Organic Matter Composition in the Solomon and Bismarck Seas (Southwest Pacific). PLoS One **10:** 19. doi:10.1371/journal.pone.0143775

Bombar, D., R. W. Paerl, R. Anderson, and L. Riemann. 2018. Filtration via Conventional Glass Fiber Filters in $^{15}N_2$ Tracer Assays Fails to Capture All Nitrogen-Fixing Prokaryotes. Frontiers in Marine Science **5:** 6. doi:10.3389/fmars.2018.00006

Bonnet, S. and others. 2013. Aphotic N_2 Fixation in the Eastern Tropical South Pacific Ocean. PLoS One **8:** 14. doi:10.1371/journal.pone.0081265

Codispoti, L. A., J. A. Brandes, J. P. Christensen, A. H. Devol, S. W. A. Naqvi, H. W. Paerl, and T. Yoshinari. 2001. The oceanic fixed nitrogen and nitrous oxide budgets: Moving targets as we enter the anthropocene? Scientia Marina **65:** 85-105.

Codispoti, L. A. 2007. An oceanic fixed nitrogen sink exceeding 400 Tg N a^{-1} vs the concept of

homeostasis in the fixed-nitrogen inventory. Biogeosciences **4:** 233-253.

Dabundo, R., M. F. Lehmann, L. Treibergs, C. R. Tobias, M. A. Altabet, P. H. Moisander, and J. Granger. 2014. The Contamination of Commercial $^{15}N_2$ Gas Stocks with ^{15}N-Labeled Nitrate and Ammonium and Consequences for Nitrogen Fixation Measurements. PLoS One **9:** e110335. doi:10.1371/journal.pone.0110335

Dang, H. Y. and others 2013. Environment-Dependent Distribution of the Sediment *nifH*-Harboring Microbiota in the Northern South China Sea. Appl. Environ. Microbiol. **79:** 121-132. doi:10.1128/aem.01889-12

Dekaezemacker, J., and S. Bonnet. 2011. Sensitivity of N_2 fixation to combined nitrogen forms (NO_3^- and NH_4^+) in two strains of the marine diazotroph *Crocosphaera watsonii* (Cyanobacteria). Mar. Ecol.-Prog. Ser. **438:** 33-46. doi:10.3354/meps09297

Dekaezemacker, J., S. Bonnet, O. Grosso, T. Moutin, M. Bressac, and D. G. Capone. 2013. Evidence of active dinitrogen fixation in surface waters of the eastern tropical South Pacific during El Niño and La Niña events and evaluation of its potential nutrient controls. Glob. Biogeochem. Cycle **27:** 768-779. doi:10.1002/gbc.20063

Deutsch, C., J. L. Sarmiento, D. M. Sigman, N. Gruber, and J. P. Dunne. 2007. Spatial coupling of nitrogen inputs and losses in the ocean. Nature **445:** 163-167.

Dutkiewicz, S., B. A. Ward, F. Monteiro, and M. J. Follows. 2012. Interconnection of nitrogen fixers and iron in the Pacific Ocean: Theory and numerical simulations. Glob. Biogeochem. Cycle **26:** 16. doi:10.1029/2011gb004039

Eyre, B. D., S. Rysgaard, T. Dalsgaard, and P. B. Christensen. 2002. Comparison of isotope pairing and N_2:Ar methods for measuring sediment-denitrification-assumptions, modifications, and implications. Estuaries **25:** 1077-1087.

Fernandez, C., L. Farias, and M. E. Alcaman. 2009. Primary production and nitrogen regeneration processes in surface waters of the Peruvian upwelling system. Prog. Oceanogr. **83:** 159-168. doi:10.1016/j.pocean.2009.07.010

Fernandez, C., L. Farias, and O. Ulloa. 2011. Nitrogen Fixation in Denitrified Marine Waters. PLoS One **6:** e20539. doi:10.1371/journal.pone.0020539

Fernandez, C., M. L. Gonzalez, C. Munoz, V. Molina, and L. Farias. 2015. Temporal and spatial variability of biological nitrogen fixation off the upwelling system of central Chile (35-38.5 degrees S). Journal of Geophysical Research-Oceans **120:** 3330-3349. doi:10.1002/2014jc010410

Gordon, L. I., J. C. Jennings Jr, A. A. Ross, and J. M. Krest. 1994. A suggested protocol for continuous flow automated analysis of seawater nutrients (phosphate, nitrate, nitrite and silicic acid) in the WOCE Hydrographic Program and the Joint Global Ocean Fluxes Study. WHP Operations and Methods. Methods Manual 91-1. November.

Großkopf, T., and J. LaRoche. 2012. Direct and indirect costs of dinitrogen fixation in *Crocosphaera watsonii* WH8501 and possible implications for the nitrogen cycle. Frontiers in Microbiology **3:** 1-10.

Großkopf, T. and others 2012. Doubling of marine dinitrogen-fixation rates based on direct

measurements. Nature **488:** 361-364. doi:10.1038/nature11338

Gruber, N. 2004. The dynamics of the marine nitrogen cycle and its influence on atmospheric CO_2 variations, p. 97-148. *In* M. Follows and T. Oguz [eds.], The Ocean Carbon Cycle and Climate. NATO - ASI Series. Kluwer Academic.

Jayakumar, A., G. D. O'Mullan, S. W. A. Naqvi, and B. B. Ward. 2009. Denitrifying bacterial community composition changes associated with stages of denitrification in oxygen minimum zones. Microb. Ecol. **58:** 350-362. doi:10.1007/s00248-009-9487-y

Jayakumar, A., M. M. D. Al-Rshaidat, B. B. Ward, and M. R. Mulholland. 2012. Diversity, distribution, and expression of diazotroph nifH genes in oxygen-deficient waters of the Arabian Sea. FEMS Microbiol. Ecol. **82:** 597-606. doi:10.1111/j.1574-6941.2012.01430.x

Jayakumar, A., B. X. Chang, B. Widner, P. Bernhardt, M. R. Mulholland, and B. B. Ward. 2017. Biological nitrogen fixation in the oxygen-minimum region of the eastern tropical North Pacific Ocean. Isme J. **11:** 2356-2367. doi:10.1038/ismej.2017.97

Karl, D. and others 2002. Dinitrogen fixation in the world's oceans. Biogeochemistry **57:** 47-98.

Kienast, M. 2000. Unchanged nitrogen isotopic composition of organic matter in the South China Sea during the last climatic cycle: Global implications. Paleoceanography **15:** 244-253.

Klawonn, I., G. Lavik, P. Boning, H. K. Marchant, J. Dekaezemacker, W. Mohr, and H. Ploug. 2015. Simple approach for the preparation of $^{15\text{-}15}N_2$-enriched water for nitrogen fixation

assessments: evaluation, application and recommendations. Frontiers in Microbiology **6:** 769. doi:10.3389/fmicb.2015.00769

Knapp, A. N., J. Dekaezemacker, S. Bonnet, J. A. Sohm, and D. G. Capone. 2012. Sensitivity of *Trichodesmium erythraeum* and *Crocosphaera watsonii* abundance and N_2 fixation rates to varying NO_3^- and PO_4^{3-} concentrations in batch cultures. Aquat. Microb. Ecol. **66:** 223-236. doi:10.3354/ame01577

Knapp, A. N., K. L. Casciotti, W. M. Berelson, M. G. Prokopenko, and D. G. Capone. 2016. Low rates of nitrogen fixation in eastern tropical South Pacific surface waters. Proc. Natl. Acad. Sci. U. S. A. **113:** 4398-4403. doi:10.1073/pnas.1515641113

Landolfi, A., P. Kahler, W. Koeve, and A. Oschlies. 2018. Global marine N_2 fixation estimates: From observations to models. Frontiers in Microbiology **9:** 8. doi:10.3389/fmicb.2018.02112

Loescher, C. R. and others 2014. Facets of diazotrophy in the oxygen minimum zone waters off Peru. Isme J. **8:** 2180-2192. doi:10.1038/ismej.2014.71

Löscher, C. R. and others 2016. N_2 fixation in eddies of the eastern tropical South Pacific Ocean. Biogeosciences **13:** 2889-2899. doi:10.5194/bg-13-2889-2016

Luo, Y. W. and others 2012. Database of diazotrophs in global ocean: abundance, biomass and nitrogen fixation rates. Earth Syst. Sci. Data **4:** 47-73. doi:10.5194/essd-4-47-2012

Luo, Y. W., I. D. Lima, D. M. Karl, C. A. Deutsch, and S. C. Doney. 2014. Data-based assessment of environmental controls on global marine nitrogen fixation. Biogeosciences

11: 691-708. doi:10.5194/bg-11-691-2014

Mahaffey, C., A. F. Michaels, and D. G. Capone. 2005. The conundrum of marine N_2 fixation. Am. J. Sci. **305:** 546-595. doi:10.2475/ajs.305.6-8.546

McElroy, M. B. 1983. Marine biological controls on atmospheric CO_2 and climate. Nature **302:** 328-329.

McIlvin, M. R., and K. L. Casciotti. 2010. Fully automated system for stable isotopic analyses of dissolved nitrous oxide at natural abundance levels. Limnol. Oceanogr. Meth. **8:** 54-66.

Mehta, M. P., D. A. Butterfield, and J. A. Baross. 2003. Phylogenetic diversity of nitrogenase (*nifH*) genes in deep-sea and hydrothermal vent environments of the Juan de Fuca ridge. Appl. Environ. Microbiol. **69:** 960-970. doi:10.1128/aem.69.2.960-970.2003

Mohr, W., T. Grosskopf, D. W. R. Wallace, and J. LaRoche. 2010. Methodological underestimation of oceanic nitrogen fixation rates. PLoS One **5:** e12583. doi:10.1371/journal.pone.0012583

Moisander, P. H., M. Benavides, S. Bonnet, I. Berman-Frank, A. E. White, and L. Riemann. 2017. Chasing after Non-cyanobacterial Nitrogen Fixation in Marine Pelagic Environments. Frontiers in Microbiology **8:** 1736. doi:10.3389/fmicb.2017.01736

Montoya, J. P., M. Voss, P. Kahler, and D. G. Capone. 1996. A simple, high-precision, high-sensitivity tracer assay for N_2 fixation. Appl. Environ. Microbiol. **62:** 986-993.

Moore, J. K., S. C. Doney, and K. Lindsay. 2004. Upper ocean ecosystem dynamics and iron

cycling in a global three-dimensional model. Glob. Biogeochem. Cycle **18:** 21. doi:10.1029/2004gb002220

Moran, S. B., M. A. Charette, S. M. Pike, and C. A. Wicklund. 1999. Differences in seawater particulate organic carbon concentration in samples collected using small- and large-volume methods: the importance of DOC adsorption to the filter blank. Mar. Chem. **67:** 33-42. doi:10.1016/s0304-4203(99)00047-x

Mulholland, M. R., K. Ohki, and D. G. Capone. 2001. Nutrient controls on nitrogen uptake and metabolism by natural populations and cultures of *Trichodesmium* (Cyanobacteria). J. Phycol. **37:** 1001-1009. doi:10.1046/j.1529-8817.2001.00080.x

Mulholland, M. R., P. W. Bernhardt, C. A. Heil, D. A. Bronk, and J. M. O'Neil. 2006. Nitrogen fixation and release of fixed nitrogen by *Trichodesmium* spp. in the Gulf of Mexico. Limnol. Oceanogr. **51:** 1762-1776. doi:10.4319/lo.2006.51.4.1762

Mulholland, M. R. and others 2012. Rates of dinitrogen fixation and the abundance of diazotrophs in North American coastal waters between Cape Hatteras and Georges Bank. Limnol. Oceanogr. **57:** 1067-1083. doi:10.4319/lo.2012.57.4.1067

Ripp, J. 1996. Analytical Detection Limit Guidance & Laboratory Guide for Determining Method Detection Limits. PUBL-TS-056-96. Wisconsin Department of Natural Resources, Laboratory Certification Program.

Sarmiento, J. L., and N. Gruber. 2006. Ocean Biogeochemical Dynamics. Princeton University Press.

Schloss, P. D. and others 2009. Introducing mothur: Open-Source, Platform-Independent, Community-Supported Software for Describing and Comparing Microbial Communities. Appl. Environ. Microbiol. **75:** 7537-7541. doi:10.1128/aem.01541-09

Smith, C. J., D. G. Nedwell, L. F. Dong, and A. M. Osborn. 2006. Evaluation of quantitative polymerase chain reaction-based approaches for determining gene copy and gene transcript numbers in environmental samples. Environmental Microbiology. **8:** 804-815. doi:10.1111/j.1462-2920.2005.00963.x

Sohm, J. A., E. A. Webb, and D. G. Capone. 2011. Emerging patterns of marine nitrogen fixation. Nat. Rev. Microbiol. **9:** 499-508. doi:10.1038/nrmicro2594

Thompson, J. D., T. J. Gibson, F. Plewniak, F. Jeanmougin, and D. G. Higgins, 1997. The CLUSTAL_X windows interface: flexible strategies for multiple sequence alignment aided by quality analysis tools. Nucleic Acids Research **25**: 4876-4882. doi:10.1093/nar/25.24.4876

Turk-Kubo, K. A., M. Karamchandani, D. G. Capone, and J. P. Zehr. 2014. The paradox of marine heterotrophic nitrogen fixation: abundances of heterotrophic diazotrophs do not account for nitrogen fixation rates in the Eastern Tropical South Pacific. Environmental Microbiology **16:** 3095-3114. doi:10.1111/1462-2920.12346

Turnewitsch, R. and others 2007. Determination of particulate organic carbon (POC) in

seawater: The relative methodological importance of artificial gains and losses in two glass-fiber-filter-based techniques. Mar. Chem. **105:** 208-228. doi:10.1016/j.marchem.2007.01.017

Voss, M., J. W. Dippner, and J. P. Montoya. 2001. Nitrogen isotope patterns in the oxygen-deficient waters of the Eastern Tropical North Pacific Ocean. Deep-Sea Res. Part I-Oceanogr. Res. Pap. **48:** 1905-1921.

Wannicke, N., M. Benavides, T. Dalsgaard, J. W. Dippner, J. P. Montoya, and M. Voss. 2018. New Perspectives on Nitrogen Fixation Measurements Using $^{15}N_2$ Gas. Frontiers in Marine Science **5**. doi:10.3389/fmars.2018.00120

White, A. E., R. A. Foster, C. R. Benitez-Nelson, P. Masque, E. Verdeny, B. N. Popp, K. E. Arthur, and F. G. Prahl. 2013. Nitrogen fixation in the Gulf of California and the Eastern Tropical North Pacific. Prog. Oceanogr. **109:** 1-17. doi:10.1016/j.pocean.2012.09.002

Widner, B., C. W. Mordy, and M. R. Mulholland. 2018. Cyanate distribution and uptake above and within the Eastern Tropical South Pacific oxygen deficient zone. Limnol. Oceanogr. **63:** S177-S192. doi:10.1002/lno.10730

Zani, S., M. T. Mellon, J. L. Collier, and J. P. Zehr. 2000. Expression of *nifH* genes in natural microbial assemblages in Lake George, New York, detected by reverse transcriptase PCR. Appl. Environ. Microbiol. **66:** 3119-3124.

Zehr, J. P., L. L. Crumbliss, M. J. Church, E. O. Omoregie, and B. D. Jenkins. 2003. Nitrogenase

genes in PCR and RT-PCR reagents: implications for studies of diversity of functional genes. Biotechniques **35:** 996-1002.

Zehr, J. P., and L. A. McReynolds. 1989. Use of degenerate oligonucleotides for amplification of the *nifH* gene from the marnine cyanobacterium *Trichodesmium thiebautii*. Appl. Environ. Microbiol. **55:** 2522-2526.

Zehr, J. P., M. T. Mellon, and S. Zani. 1998. New nitrogen-fixing microorganisms detected in oligotrophic oceans by amplification of nitrogenase (*nifH*) genes. Appl. Environ. Microbiol. **64:** 3444-3450.

Figure legends

Figure 1. Map of study area. Filled black circles are locations of N_2 fixation experiments overlain on satellite-derived surface chlorophyll a concentrations (mg m^{-3}). Chlorophyll a data is from NASA MODIS Aqua (mean concentration for June 2013).

Figure 2. Hydrographic data and N_2 fixation rates in study area. Top panels are ODZ margin stations (Sta. 2 and 10). Middle panels are offshore ODZ stations (Sta. BB1, 9, and 16). Bottom panels are coastal stations (Sta. 21 and BB2). Legends in right panels apply to all panels in row. Left panels are profiles of $[O_2]$ (μmol kg^{-1}). Middle panels are $[NO_3^-]$, $[NO_2^-]$, and $[NH_4^+]$ (μmol kg^{-1}). Right panels are N_2 fixation rates (nmol L^{-1} d^{-1}) at Sta. 2, 10, BB1, 9, 16, 21, and BB2. Error bars are ±1 SD (n =3). N_2 fixation rates above detection limit outlined in red.

Figure 3. Abundance of *nifH* copies (*nifH* copies mL^{-1}) at: A) Sta. BB1 and B) Sta. BB2. Error bars are ±1 SD (n = 3).

Figure 4. N_2 fixation rates above detection limit only (nmol L^{-1} d^{-1}) vs. [DIN] (μmol kg^{-1}). Error bars are ±1 SD (n =3).

Table 1. Hydrographic regimes in this study.

		Euphotic zone			ODZ	
Regime	Station	$[NO_3^-]$ (μmol kg^{-1})	$[NH_4^+]$ (μmol kg^{-1})	[Chl a] (mg m^{-3})	ODZ thickness (m)	2° NO_2^- max (μmol kg^{-1})
ODZ margin	2, 10	0.3 – 0.6	below detection – 0.1	0.1 – 0.4	<30	0
Offshore ODZ	BB1, 9, 16	1.0 – 2.3	0.1 – 0.4	0.1 – 2.3	~250	>7
Coastal ODZ	21, BB2	2.7 – 7.3	0.3 – 0.6	0.3 – 5.6	~330	>7

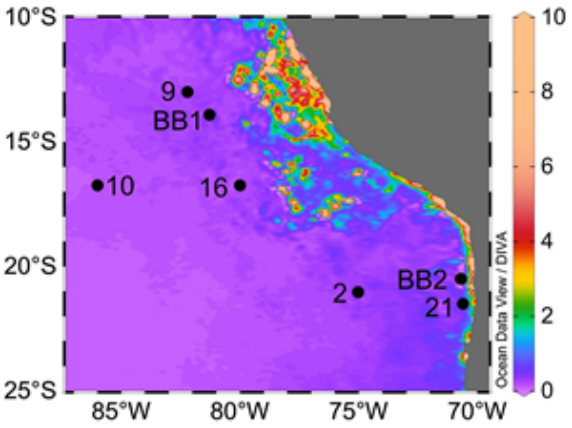

Figure 1

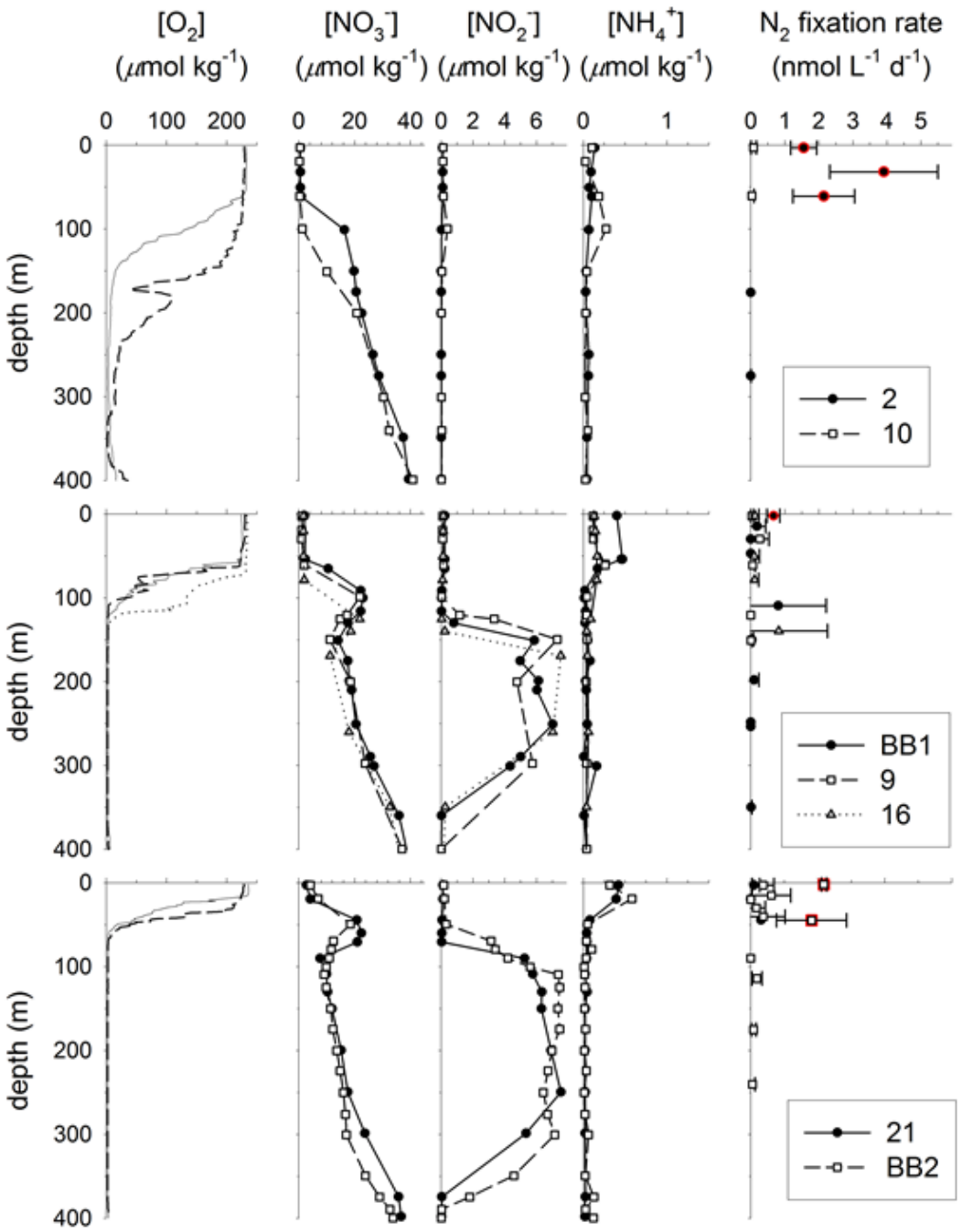

Figure 2

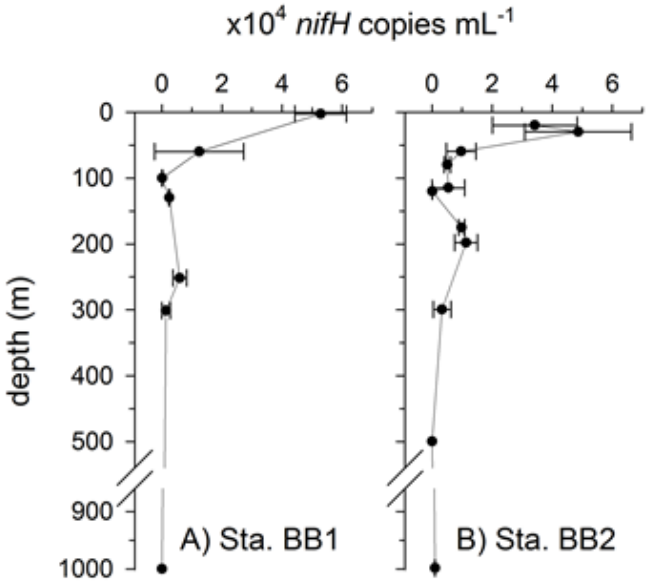

Figure 3

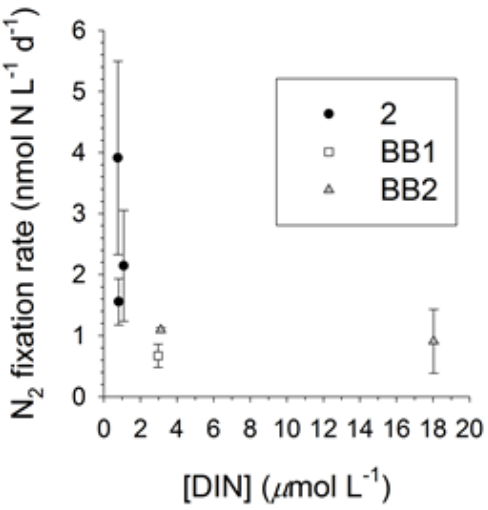

Figure 4. N_2 fixation rates above detection limit only (nmol L^{-1} d^{-1}) vs. [DIN] (μmol kg^{-1}). Error bars are ±1 SD (n =3).

Table 1. Hydrographic regimes in this study.

		Euphotic zone			ODZ	
Regime	Station	$[NO_3^-]$ (μmol kg^{-1})	$[NH_4^+]$ (μmol kg^{-1})	[Chl a] (mg m^{-3})	ODZ thickness (m)	2° NO_2^- max (μmol kg^{-1})
ODZ margin	2, 10	0.3 – 0.6	below detection – 0.1	0.1 – 0.4	<30	0
Offshore ODZ	BB1, 9, 16	1.0 – 2.3	0.1 – 0.4	0.1 – 2.3	~250	>7
Coastal ODZ	21, BB2	2.7 – 7.3	0.3 – 0.6	0.3 – 5.6	~330	>7